Small Molecule Adsorption on Defective Phosphorene

A. S. Giraldo-Neira *, C. A. Duque *, A. L. Morales, J. D. Correa *, M. E. Mora-Ramos

Posted Date: 4 February 2026

doi: 10.20944/preprints202602.0338.v1

Keywords: black phosphorene; single and double vacancies; small gas molecule adsorption; density functional theory

 doi:10.20944/preprints202602.0338.v1

Article

Small Molecule Adsorption on Defective Phosphorene

A. S. Giraldo-Neira [1,*], C. A. Duque [1,*], A. L. Morales [1], J. D. Correa [2,*] and M. E. Mora-Ramos [3]

[1] Grupo de Materia Condensada-UdeA, Instituto de Física, Facultad de Ciencias Exactas y Naturales, Universidad de Antioquia UdeA, Calle 70 No. 52-21, Medellín, Colombia
[2] Instituto de Ciencias Básicas, Facultad de Ingenierías, Universidad de Medellín, Medellín,Colombia
[3] Centro de Investigación en Ciencias-IICBA, Universidad Autónoma del Estado de Morelos, Av. Universidad 1001, CP 62209 Cuernavaca, Morelos, México
* Correspondence: anna.giraldo@udea.edu.co (A.S.G.-N.); carlos.duque1@udea.edu.co (C.A.D.); jcorrea@udemedellin.edu.co (J.D.C.)

Abstract

We perform Density Functional Theory calculations to determine adsorption energies of small gas molecules (H_2, N_2, NO, and CO) on defective, vacancy-laden, black phosphorene. Different configurations of single and double vacancies in the monolayer structure are considered, together with several possible adsorption sites onto them. The van der Waals interaction is considered for the exchange-correlation functional. This research aims to provide fundamental insights into how atomic vacancies can be engineered to tune phosphorene's surface reactivity, offering a broader understanding of its multifaceted applications.

Keywords: black phosphorene; single and double vacancies; small gas molecule adsorption; density functional theory

1. Introduction

The isolation of graphene in 2004 established a new paradigm in materials science, facilitating the broad investigation of atomically thin materials [1–4]. Within the search for alternative 2D systems, black phosphorus has attracted significant attention, particularly in its monolayer allotrope, phosphorene [5]. In contrast to semi-metallic graphene, phosphorene (also called black phosphorene) exhibits a direct and tunable band gap, a property that makes it suitable for optoelectronic applications, such as field-effect transistors (FETs) with substantial on/off ratios [6–8]. Furthermore, its puckered honeycomb lattice results in strong anisotropy in relation to its electronic, optical, and thermal properties, a characteristic that has motivated significant research [9–13]. Recent studies have examined the utility of functional phosphorene in diverse areas, including supercapacitors and nanotherapeutic platforms [14–16].

Despite its remarkable potential, the practical implementation of phosphorene is constrained by its inherent instability at ambient conditions. The presence of lone-pair of electrons on the phosphorus atoms heightens chemical reactivity, precipitating degradation upon exposure to oxygen and moisture [17]. However, this intrinsic reactivity invites a paradigm shift towards "defect engineering." Far from being regarded as merely structural aberrations, atomic vacancies are increasingly recognized as mechanisms to precisely modulate material properties at the atomic scale [18,19]. Theoretical frameworks suggest that native vacancies fundamentally reshape the electronic landscape, introducing localized in-gap states and inducing magnetism in the otherwise non-magnetic lattice [20–22]. Notably, single and double vacancies stabilize in anionic (-1) charge states, altering local geometries; while these defects may lower the energy barrier for oxidative degradation via O_2 dissociation [23], they concurrently offer significant tunability. For example, vacancy-induced magnetic moments can be manipulated by doping with elements such as N, Fe, or Co [24], while the emergence of quasi-flat states near the Fermi level significantly influences optical responses [25].

 doi:10.20944/preprints202602.0338.v1

This ability to tailor the surface reactivity is particularly pertinent to gas-sensing applications. Pristine phosphorene is generally limited by weak physisorption interactions with common analytes, resulting in suboptimal sensitivity [26]. Defect engineering addresses this limitation by introducing active sites—such as vacancies or heteroatom substitutions—that enhance the adsorption strength. While mono- and di-vacancy defects significantly augment gas adsorption, it is noted that the resulting electronic perturbations must be carefully managed to ensure sufficient sensitivity [27]. As it turns out, when optimized, defective phosphorene not only improves adsorption kinetics but also preserves the material's stability and reusability, solidifying its promise for sensing platforms [28].

First-principles calculations have long predicted that phosphorene could surpass other 2D materials in sensing performance 00[29,30]. The underlying hypothesis posits that structural defects function as reactive centers, facilitating a transition from physisorption to chemisorption characterized by substantial charge transfer. This mechanism is well-documented in analogous systems; for example, vacancies in graphene markedly enhance sensitivity to NO_2 [31], while specific defect configurations in Tin Monosulfide (SnS) enable tunable selectivity [32]. Similarly, single vacancies in blue phosphorene have been shown to drastically strengthen interactions with pollutant molecules [33].

Despite these advances, a systematic understanding of how specific vacancy configurations in phosphorene govern interactions with small, environmentally relevant molecules remains elusive. Critical questions persist regarding the comparative efficacy of single vacancies (SV) versus double vacancies (DV), and how distinct defect geometries influence the adsorption mechanisms for simple diatomic molecules. Addressing this lack of fundamental comparative insight is essential for overcoming current bottlenecks and designing phosphorene-based sensors with tailored selectivity.

This is precisely the void that the present study aims to fill. Using the SIESTA package, which is based on Density Functional Theory [34], we rigorously investigate the adsorption of key molecules such as H_2, N_2, NO, and CO [35]. Our focus is on three surface types: phosphorene with a single vacancy (SV) and two distinct double vacancy (DV) configurations, consistent with the comparison of the results against the pristine phosphorene case. To ensure the precision of the adsorption calculations, the van der Waals interaction is explicitly included in the exchange-correlation functional [36]. The ultimate goal is to provide a detailed understanding of how structural defects govern adsorption, providing a critical piece of the puzzle to unleash the multifaceted potential of phosphorene in chemical sensing.

2. Methodology

Our study employs first-principles calculations within the framework of Density Functional Theory (DFT), using the SIESTA code [34] for all simulations, while the Atomic Simulation Environment (ASE) library [37] was used for workflow management and structural setup. To accurately describe exchange-correlation interactions, particularly the dispersive forces relevant to adsorption, we included the KBM van der Waals functional [36]. The core electrons of the phosphorus atoms were described using norm-conserving pseudopotentials optimized for the KBM functional. Valence states were expanded using a linear combination of numerical atomic orbitals with a double-zeta polarized (DZP) basis set. The spatial precision was defined by a basis-set confinement energy shift of 0.1 eV and a real-space grid cutoff of 250 Ry. Structural relaxations were performed using the conjugate gradient method until the maximum force component on any atom was less than $0.04\,\mathrm{eV}/$. For the Brillouin zone integration, a $10 \times 10 \times 1$ Monkhorst-Pack grid was employed for the unit cell, while a $1 \times 1 \times 1$ sampling (Γ-point) was used for supercell partition. Additionally, spin-polarized calculations were enabled to evaluate the total magnetization in cases where adsorption induces unpaired magnetic moments in the molecule-phosphorene complex.

To model the adsorption surfaces, we constructed a 7×5 rectangular phosphorene supercell. Based on this geometry, four distinct systems were generated to assess the impact of structural defects, as schematically shown in Figure 1. These systems include the pristine non-defective monolayer, which serves as a baseline, and three defective configurations: the Single Vacancy (SV), formed by removing

 doi:10.20944/preprints202602.0338.v1

a single phosphorus atom; the Divacancy Type 1 (DV1), created by eliminating two neighboring phosphorus atoms located in different (top and bottom) sub-layers; and the Divacancy Type 2 (DV2), generated by removing two adjacent atoms from the same puckered sub-layer. After creating these vacancies, the geometries were fully relaxed to allow local atomic reconstruction around the defect sites.

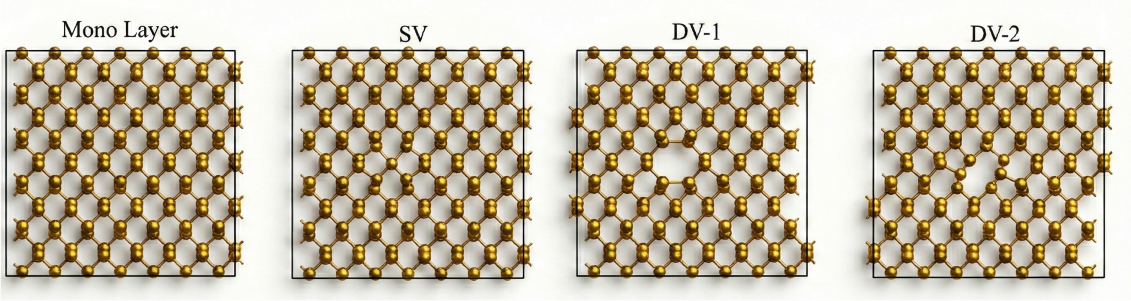

Figure 1. Schematic representation of the four phosphorene supercells studied. From left to right: the pristine (non-defective) Mono Layer; the Single Vacancy (SV) system, created by removing one P atom; the Divacancy Type 1 (DV-1), formed by removing two adjacent atoms from different sub-layers; and the Divacancy Type 2 (DV-2), formed by removing two adjacent atoms from the same sub-layer.

To quantify the stability of the interaction between molecules and the surface, the adsorption energy (E_{ads}) is calculated using the following expression.

$$E_{ads} = E_{layer} + E_{gas} - E_{total}\,, \tag{1}$$

where E_{total} corresponds to the total energy of the layer-adsorbed gas complex, E_{layer} is the energy of the isolated substrate (pristine or defective), and E_{gas} is the energy of the isolated gas phase molecule. To identify the most favorable binding configurations, we explored several potential adsorption sites as illustrated in Figure 2. For the pristine monolayer, high-symmetry sites were considered: the top site (directly above a P atom), the bridge site (midway between two bonded P atoms), and the hollow site (at the center of a phosphorene ring). For the defective surfaces, additional adsorption sites near the low-coordination atoms were thoroughly investigated to account for the unique geometries introduced by the vacancies.

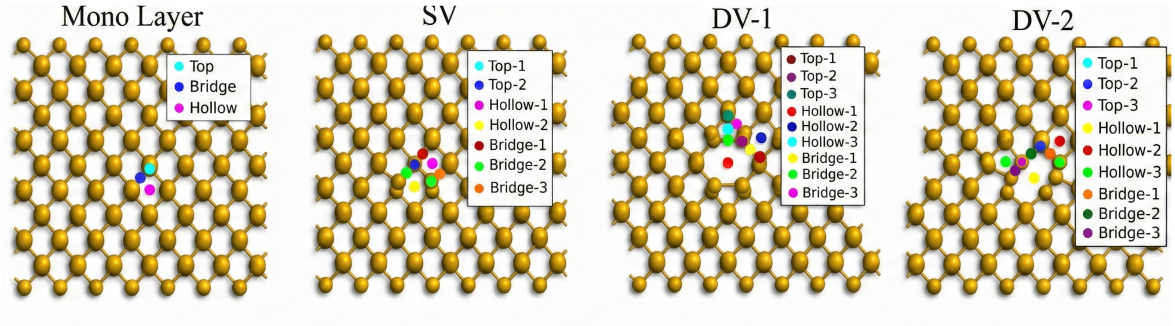

Figure 2. Top-down view of the adsorption sites investigated for small gas molecules on each phosphorene system. For the pristine Mono Layer, standard top, bridge, and hollow sites were considered. For the defective systems SV, DV-1, and DV-2), additional unique sites were explored in the immediate vicinity of the vacancy to account for the locally altered chemical environment.

 doi:10.20944/preprints202602.0338.v1

3. Result and Discussion

We first examine the electronic structure of both pristine and defective phosphorene monolayers, with the calculated band structures illustrated in Figure 3. The pristine monolayer (NV) exhibits a direct band gap of ≈ 0.9 eV at the Γ point, a result consistent with previous first-principles studies [21]. The introduction of a single vacancy (SV) breaks the lattice symmetry, leading to the emergence of a highly localized, nearly dispersionless, defect state within the forbidden region. This state is pinned at the Fermi level (0 eV) and lies approximately 0.2 eV above the valence-band maximum. Such states are expected to act as chemically active sites, facilitating molecular adsorption. A similar behavior is observed in the DV-1 configuration, mainly affecting the conduction-band interval; however, a band gap comparable to that of the pristine monolayer is preserved. In contrast, the DV-2 defect retains the semiconducting character but results in a significantly narrowed direct band gap of ≈ 0.3 eV. These findings align well with previous theoretical reports on defective phosphorene [20]. In all defective cases, a significant increase in the number of valence or conduction band states within the same energy interval is observed. These distinct electronic signatures demonstrate that specific defect topologies and coordination environments modulate the material's electronic landscape, a critical factor that governs subsequent interactions with gas molecules.

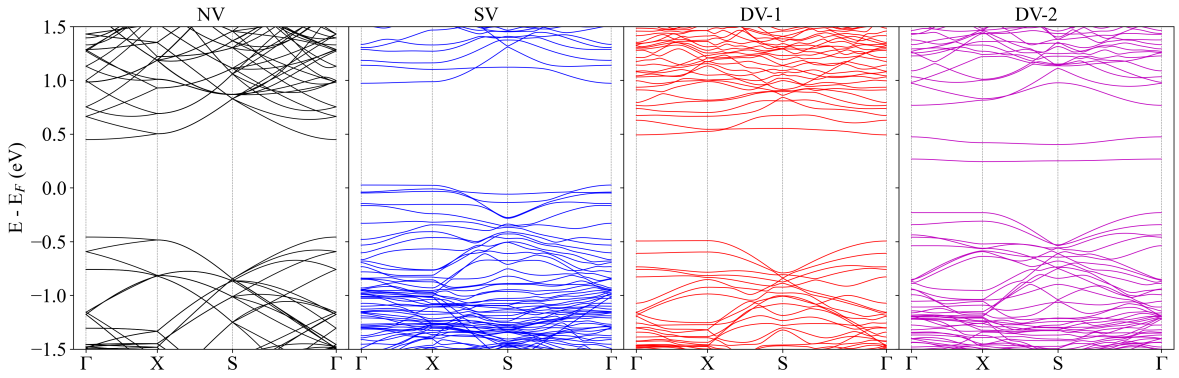

Figure 3. Band structures for pristine (NV), Single Vacancy (SV), Divacancy Type 1 (DV-1), and Divacancy Type 2 (DV-2) phosphorene monolayers.

We started by studying the adsorption of H_2, N_2, CO, and NO on the pristine phosphorene monolayer to establish a baseline for comparison. For the polar molecules CO and NO, we considered two distinct orientations: with the oxygen atom pointing towards the surface (**v1**) and with the carbon/nitrogen atom pointing towards the surface (**v2**). The calculated adsorption energies (E_{ad}) and molecular bond lengths are summarized in Table 1.

Table 1. Adsorption energies (E_{ad} in eV) and bond lengths (d in Å) for various molecules on pristine black phosphorene.

Molecule	Hollow		Bridge		Top	
	E_{ad}	d	E_{ad}	d	E_{ad}	d
H_2	-0.057	0.778	-0.058	0.778	-0.048	0.778
N_2	-0.031	1.118	-0.042	1.119	-0.060	1.119
CO-v1	-0.009	1.151	0.021	1.151	0.019	1.152
NO-v1	-0.391	1.178	-0.383	1.179	-0.341	1.179
CO-v2	0.039	1.151	0.016	1.151	0.007	1.152
NO-v2	-0.396	1.182	-0.374	1.183	-0.396	1.185

In general, all configurations exhibit characteristic traits of weak physisorption. The strongest attractive interaction is observed for NO at the top site, yielding a E_{ad} of only −396 meV. For NO, molecular orientation plays a noticeable role; specifically, the configuration with the oxygen atom closer to the surface (NO-v1) is energetically more favorable. In stark contrast, the interaction with the CO molecule is found to be repulsive (positive E_{ad}) or negligible for both v1 and v2 orientations, indicating

 doi:10.20944/preprints202602.0338.v1

that pristine phosphorene has a negligible affinity for carbon monoxide regardless of its orientation. Regarding the H_2 molecule, the adsorption energies display typical small values reported for other 2D nanomaterials, such as defective graphene doped with B/N, which exhibits adsorption energies ranging from -0.009 to -0.080 eV depending on molecular orientation [13]. This weak-interaction nature is further corroborated by analysis of intramolecular bond lengths. For all adsorbed molecules, these bond lengths remain largely unperturbed, showing minimal variation across different adsorption sites and orientations. Collectively, these findings confirm that the interactions are governed by van der Waals forces with negligible charge transfer, establishing the pristine phosphorene monolayer as an ineffective substrate for the sensing of these small gas molecules.

To enhance the adsorption properties of phosphorene, we systematically evaluated the interaction of gas molecules within the vicinity of the three defective structures illustrated in Figure 1, considering all adsorption positions detailed in Figure 2. Figure 4 summarizes the maximal absolute adsorption energy ($|E_{ad}|$) calculated for each molecule in different structural configurations.

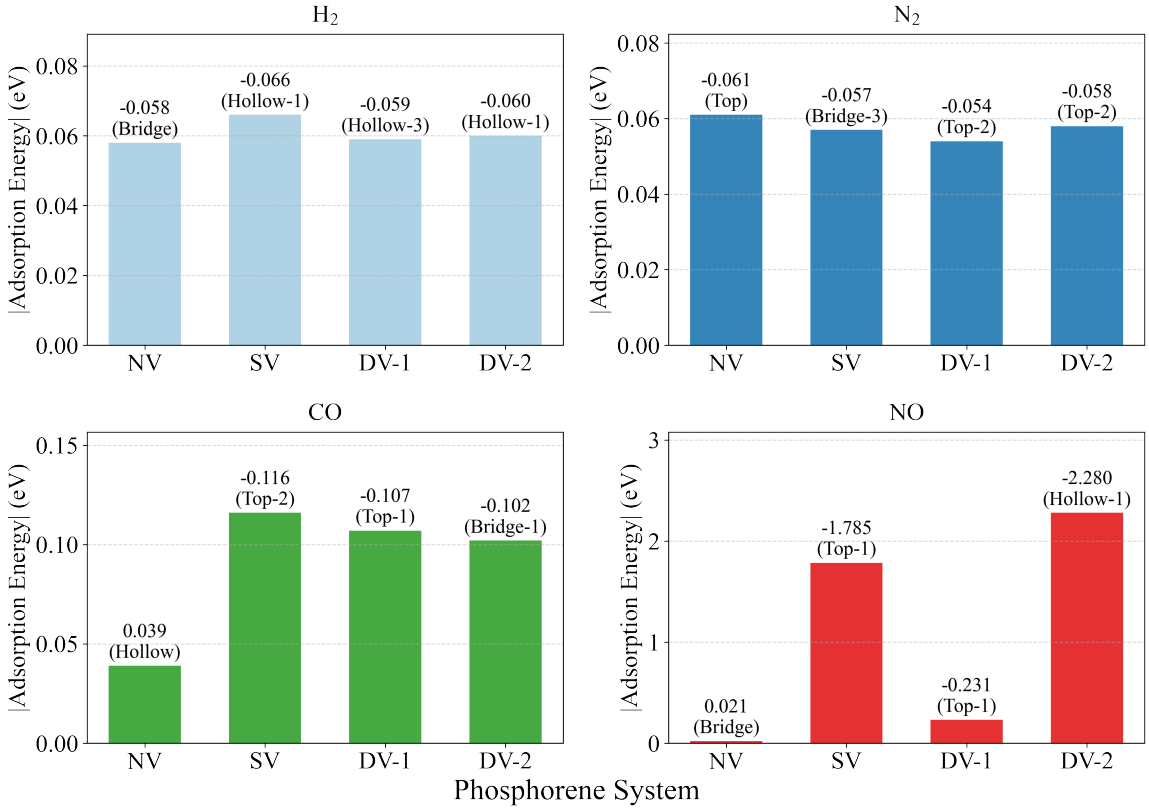

Figure 4. Absolute adsorption energy ($|E_{ad}|$ in eV) for H_2, N_2, CO, and NO molecules on Pristine (NV), Single Vacancy (SV), Divacancy Type 1 (DV-1), and Divacancy Type 2 (DV-2) black phosphorene monolayers. The height of the bars represents the absolute magnitude, while the labels above indicate the exact calculated adsorption energy values and the corresponding most stable adsorption site.

For homonuclear diatomic molecules, H_2 and N_2, the adsorption energetics are largely insensitive to surface defects. As shown in Figure 4, the maximal adsorption energy for H_2 remains comparable between the pristine and defective monolayers, peaking slightly at -0.066 eV in the Single Vacancy (SV) system (Hollow-1 site). A similar trend is observed for N_2, which exhibits a consistent adsorption energy hovering around -0.060 eV regardless of the type of defect. These low energy values indicate

 doi:10.20944/preprints202602.0338.v1

a physisorption mechanism dominated by weak van der Waals interactions, suggesting that neither pristine nor defective phosphorene significantly retains these gases.

In contrast, the adsorption behavior of the heteronuclear molecules, CO and NO, is strongly influenced by the surface topology. Structural defects significantly enhance the interaction strength for these species. For CO, the maximal adsorption energy increases from -0.039 eV on the pristine surface to -0.116 eV in the presence of a Single Vacancy (SV, Top-2 site). The effect is most pronounced for NO, where the introduction of defects triggers a dramatic transition from weak physisorption to strong chemisorption. Although NO is weakly adsorbed on the pristine surface ($E_{ad} = -0.021$ eV), the binding energy increases to -1.785 eV for the SV system (Top-1 site) and reaches a maximum of -2.280 eV for the Divacancy Type 2 (DV-2) system (Hollow-1 site). A comprehensive analysis of the adsorption energies, including values for all considered positions, is provided in the Supplementary Material.

The analysis suggests that while most gas molecules (H_2, N_2, and CO) undergo physisorption with relatively low binding energies, the NO molecule is a notable exception. The substantial energies observed for NO on defective surfaces (exceeding -1.0 eV) imply the formation of strong chemical bonds. This increased adsorption probability is likely correlated with significant structural distortions in the adsorbate, such as bond elongation, particularly at the highly active sites identified in the SV and DV-2 systems. Consequently, based on these calculations, defective phosphorene monolayers —especially those containing Single Vacancies or Type-2 Divacancies— appear to be highly suitable candidates for the capture or detection of gaseous nitric oxide.

To gain a deeper understanding of the electronic consequences of adsorption, we calculated the Total Density of States (TDOS) for the previously identified most stable configurations. Figure 5 presents the DOS for the molecule-phosphorene complexes. The shadowed gray regions at the bottom of each panel represent the reference DOS of the isolated phosphorene substrates (pristine or defective) prior to adsorption.

Upon gas adsorption, the electronic structure undergoes discernible modifications. For homonuclear molecules (H_2 and N_2), the interaction remains largely non-invasive regarding the metallicity of the system. As shown in the upper panels of Figure 5, the presence of H_2 induces a rigid shift of the energy states; however, the band gap is preserved across all defect types (NV, SV, DV-1, and DV-2), indicating that the system retains its semiconductor character with the Fermi level (E_F) located within the gap. A comparable behavior is observed for N_2, where the DOS profiles show that the semiconducting nature of the phosphorene monolayer is largely unaffected by the physical adsorption of nitrogen.

In heteronuclear molecules, the electronic response is more complex. For CO adsorption, the system generally maintains a semiconductor band gap, similar to the pristine case. However, significant changes occur with NO adsorption. The NO molecule introduces states within the band gap, and, notably, induces a symmetry breaking in the electronic states. As evidenced in the bottom-right panel of Figure 5, the DOS for NO becomes spin-polarized (asymmetry between solid and dashed lines), particularly for defective substrates. This interaction leads to the emergence of impurity states near the Fermi level, effectively doping the material.

This spin polarization is quantified in Table 2. Although adsorption of H_2, N_2, and CO results in non-magnetic ground states ($0\ \mu_B$) across all structural defects, the NO molecule induces a significant magnetic moment. This confirms that the distinct split observed in the NO DOS plots corresponds to a net magnetization arising from the unpaired electrons of the nitric oxide molecule interacting with the localized defect states of the phosphorene lattice.

 doi:10.20944/preprints202602.0338.v1

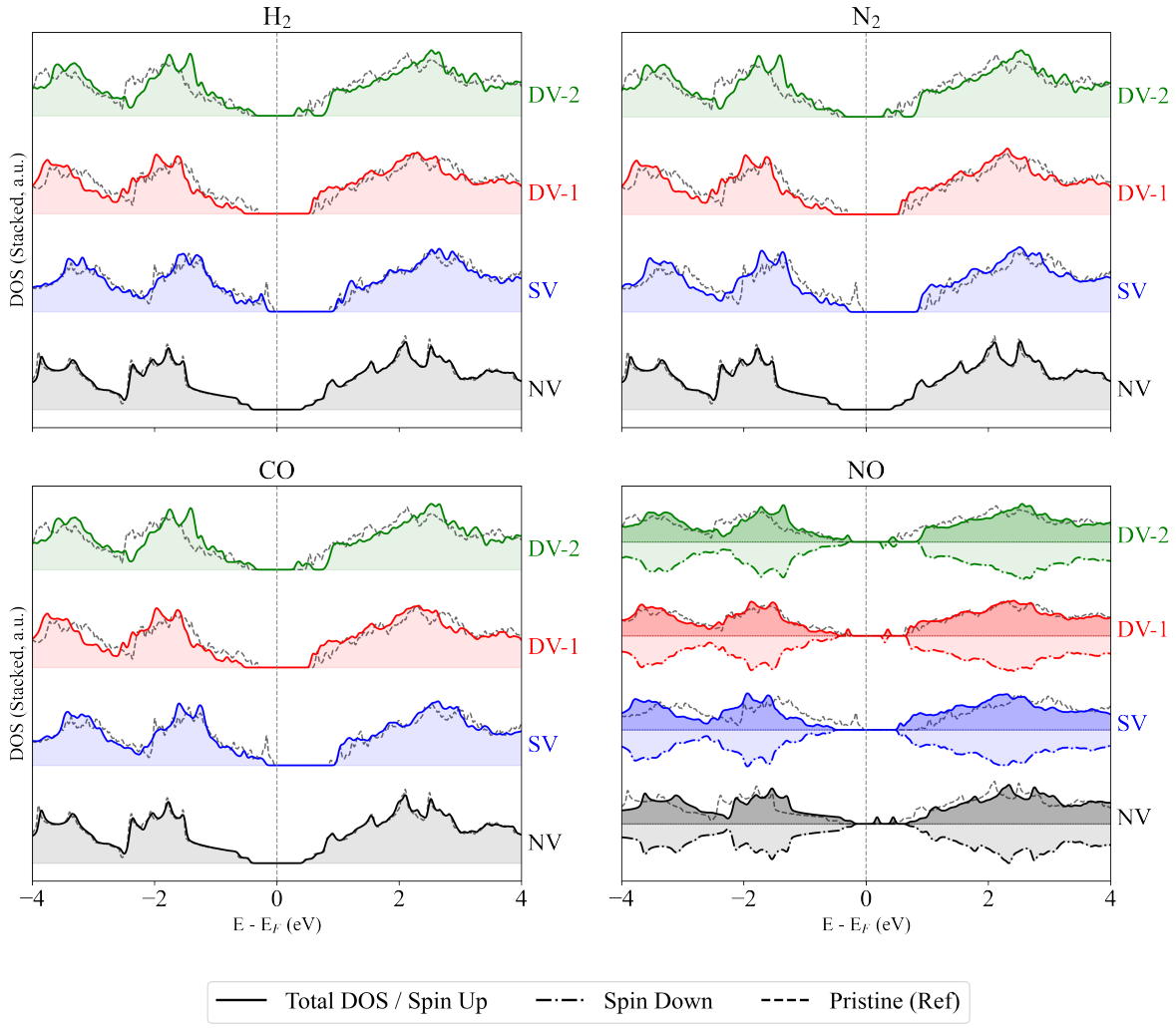

Figure 5. Calculated density of states (DOS) for all considered black phosphorene monolayer/adsorbed molecule complexes. The solid lines represent the total DOS (or Spin Up for magnetic systems), while the dash-dotted lines represent the Spin Down component, and the dashed lines represent the reference DOS for the clean substrates.

Table 2. Total magnetic moment (μ_B) for molecule adsorption at the most stable sites on defective phosphorene monolayers.

Defect Type	H_2	N_2	**CO**	**NO**
SV	0.0	0.0	0.0	1.000
DV-1	0.0	0.0	0.0	1.000
DV-2	0.0	0.0	0.0	1.000

The optical properties of the phosphorene-molecule complexes were analyzed by calculating the imaginary part of the dielectric function $\varepsilon_2(\omega)$, which is directly related to the optical absorption spectra. This analysis provides a spectroscopic signature that complements the discussion of electronic structure provided above. Figure 6 displays the absorption spectra for both X (armchair) and Y (zigzag) light polarizations, summing over spin components to capture the total optical response.

 doi:10.20944/preprints202602.0338.v1

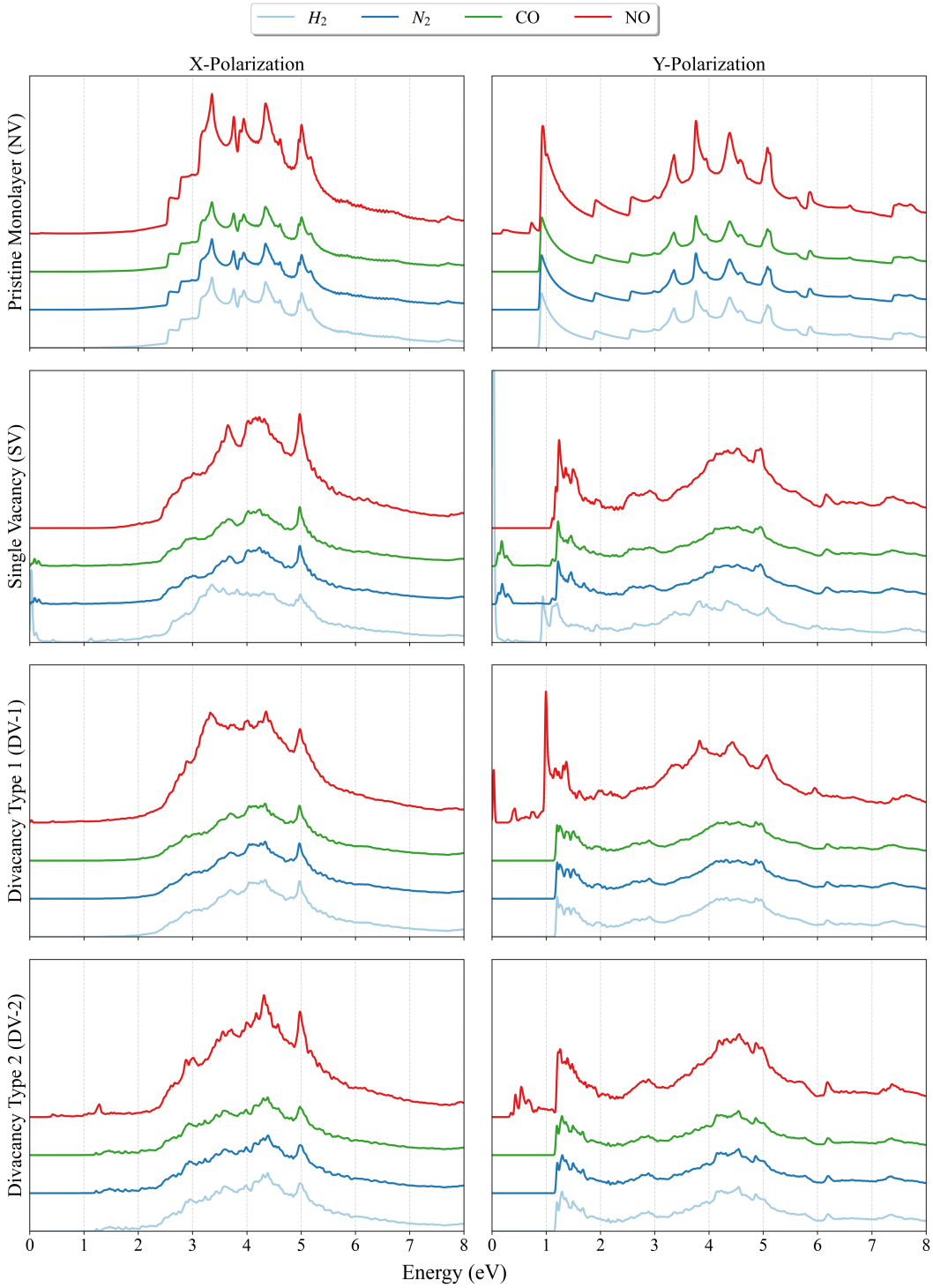

Figure 6. Calculated optical absorption spectra for H_2, N_2, CO, and NO molecules adsorbed on Pristine (NV), Single Vacancy (SV), Divacancy Type 1 (DV-1), and Divacancy Type 2 (DV-2). The left and right panels correspond to light polarized along the X-direction (armchair) and Y-direction (zigzag), respectively.

Consistent with the intrinsic anisotropy of black phosphorene, all systems exhibit a marked polarization-dependent behavior. The absorption profiles along the X-direction generally show broad absorption bands starting in the visible range, while the Y-direction is characterized by sharper features and distinct low-energy transitions.

For the physisorbed molecules (H_2, N_2) and CO, the optical spectra largely mirror the behavior of the host phosphorene lattice. As observed in Figure 6, the absorption edges for these species are located above 1.5 eV. This is in excellent agreement with the DOS analysis, where these systems were

 doi:10.20944/preprints202602.0338.v1

identified as semiconductors with preserved band gaps. The lack of optical absorption in the infrared region (< 1.0 eV) confirms that the adsorption of these gases does not introduce new intragap states capable of mediating low-energy excitations. Consequently, the optical transparency of phosphorene in the low-energy regime remains intact upon exposure to H_2, N_2, and CO.

A strikingly different behavior is observed for the NO molecule. Correlating with the DOS results, where NO adsorption induced spin-polarized impurity states within the band gap and near the Fermi level, the optical spectra exhibit distinct new absorption peaks in the low-energy range ($0.0 - 1.0$ eV). These features are particularly prominent in the Y-polarization for the defective systems (SV, DV-1, and DV-2), appearing as sharp peaks or "pre-edges" below the main absorption band. These transitions correspond to electronic excitations involving the localized mid-gap states generated by the strong chemical interaction between nitric oxide and the defective phosphorene surface. The emergence of these unique optical signatures in the infrared region suggests that optical spectroscopy could be an effective method to selectively detect NO, distinguishing it from other common gases.

4. Conclusions

We have performed DFT calculations to investigate the features of small gas-molecule adsorption on black phosphorene. In particular, we have assumed that the adsorbent surfaces can be defect-laden, with single and double atomic vacancies in the two-dimensional lattice of otherwise pristine monolayers. Given the structure's geometry, several adsorption sites can be identified, which are more numerous when double vacancies are present. In all cases, the adsorption energy was evaluated for each of the gases considered: H_2, N_2, CO, and NO. It has been found that adsorption energies tend to be small (only a few tens of meV) for three of the species included in the study. The only one that exhibits rather significant values of the adsorption energy is NO, and this happens only in the case of a defective adsorbent surface with single phosphorus atom vacancies. Here, the obtained values suggest that this particular defective substrate is suitable for practical nitric oxide capture. In addition, magnetic response due to spin polarization is predicted for NO adsorption on double-vacancy-laden black phosphorene monolayers.

Supplementary Materials: The following supporting information can be downloaded at the website of this paper posted on Preprints.org.

Author Contributions: The contributions of the authors are as follows: A.S.G.-N.: Conceptualization, Methodology, Software, Validation, Formal Analysis, Investigation, Data curation, Writing—Review and Editing, Visualization. J.D.C.: Conceptualization, Methodology, Software, Validation, Formal Analysis, Investigation, Data curation, Writing—Review and Editing, Visualization. M.E.M-R.: Conceptualization, Methodology, Software, Validation, Formal Analysis, Investigation, Data curation, Writing—Review and Editing, Visualization. A.L.M.: Conceptualization, Formal Analysis, Writing—Review and Editing, Visualization. C.A.D.: Conceptualization, Formal Analysis, Writing— Review and Editing, Visualization. All authors have read and agreed to the published version of the manuscript.

Funding: This research received no external funding.

Acknowledgments: ASGN and CAD thank the University of Antioquia for support through the Young Researchers Program fellowship. JDC and MEMR are grateful to Mexican SECIHTI for support through Grant CBF-2025-I-1058.

References

1. Novoselov, K.S.; Geim, A.K.; Morozov, S.V.; Jiang, D.; Zhang, Y.; Dubonos, S.V.; Grigorieva, I.V.; Firsov, A.A. Electric field effect in atomically thin carbon films. *Science* **2004**, 306, 666-669.
2. Tang, S.; Cao, Z. Adsorption and dissociation of ammonia on graphene oxides: A first-principles study. *J. Phys. Chem. C* **2012**, 116, 8778-8791.
3. Mattson, E.C.; Pande, K.; Unger, M.; Cui, S.; Lu, G.; Gajdardziska-Josifovska, M.; Weinert, M.; Chen, J.; Hirschmugl, C.J. Exploring adsorption and reactivity of NH3 on reduced graphene oxide. *J. Phys. Chem. C* **2013**, 117, 10698-10707.

 doi:10.20944/preprints202602.0338.v1

4. Zhu, S.; Sun, H.; Liu, X.; Zhuang, J.; Zhao, L. Room-temperature NH3 sensing of graphene oxide film and its enhanced response on the laser-textured silicon. *Sci. Rep.* **2017**, 7, 14773.
5. Batmunkh, M.; Bat-Erdene, M.; Shapter, J.G. Phosphorene and phosphorene-based materials–prospects for future applications. *Adv. Mater.* **2016**, 28, 8586-8617.
6. Li, L.; Yu, Y.; Ye, G.J.; Ge, Q.; Ou, X.; Wu, H.; Feng, D.; Chen, X.H.; Zhang, Y. Black phosphorus field-effect transistors. *Nat. Nanotechnol.* **2014**, 9, 372-377.
7. Mohammadi, M.; Tavangar, Z. Adsorption of aromatic molecules on a black phosphorene surface: A first-principles study. *New J. Chem.* **2023**, 47, 1842-1851.
8. Talukdar, D.; Mohanta, D.; Ahmed, G.A. Nitrogen doped compound defect in black phosphorene for enhanced gas sensing. *Surf. Interfaces* **2024**, 51, 104699.
9. Tariq, M.; Khattak, J.I.; Iqbal, M.; Ullah, R.; Zeb, A.; Khan, M.; Khan, A.; Mahmood, T.; Ahmad, I. DFT study of the therapeutic potential of phosphorene as a drug delivery system for chlorambucil to treat cancer. *RSC Adv.* **2019**, 9, 24325-24332.
10. Pica, M.; D'Amato, R. Chemistry of Phosphorene: Synthesis, Functionalization and Biomedical Applications in an Update Review. *Inorganics* **2020**, 8, 29.
11. Kumar, A.; Kumar, M.; Kumar, M. Recent advances in phosphorene-based gas sensors. *Sens. Actuators A Phys.* **2019**, 295, 523-537.
12. de Sousa, F.E.B. Electronic, Transport and Optical Properties in Multilayer Phosphorene. Ph.D. Thesis, Federal University of Ceará, Brazil, 2023.
13. Akilan, R.; Vinnarasi, S.; Mohanapriya, S.; Shankar, R. Adsorption of H2 molecules on B/N-doped defected graphene sheets—A DFT study. *Struct. Chem.* **2020**, 31, 2413-2434.
14. Halder, P.; Mondal, I.; Kundu, M.; Ghosh, A.; Paul, B.K.; Biswas, S.; Sau, S.; Chattopadhyay, B.; Mondal, D.; Das, S. Optimizing phosphorene nanosheets for high performance all-solid asymmetric supercapacitors: A theoretical and experimental insight. *J. Energy Storage* **2024**, 94, 112451.
15. Cui, X.; Tang, X.; Niu, Y.; Tong, L.; Zhao, H.; Yang, Y.; Jin, G.; Li, M.; Han, X. Functional phosphorene: Burgeoning generation, two-dimensional nanotherapeutic platform for oncotherapy. *Coord. Chem. Rev.* **2024**, 507, 215744.
16. Zhu, Y.; Xie, Z.; Li, J.; Liu, Y.; Li, C.; Liang, W.; Huang, W.; Kang, J.; Cheng, F.; Kang, L.; Al-Hartomy, O.A.; Al-Ghamdi, A.; Wageh, S.; Xu, J.; Li, D.; Zhang, H. From phosphorus to phosphorene: Applications in disease theranostics. *Coord. Chem. Rev.* **2021**, 446, 214110.
17. Zeng, X.; Liu, G.; Wang, W.; Wang, Y.; Liu, F.; Wu, M. Black phosphorus: Synthesis, stability, and applications. *iScience* **2021**, 24, 103116.
18. Kaewmaraya, T.; Singh, D.; Kumar, A.; Park, S.; Lee, H. Drastic Improvement in Gas-Sensing Characteristics of Phosphorene Nanosheets under Vacancy Defects and Elemental Functionalization. *J. Phys. Chem. C* **2018**, 122, 19864-19874.
19. Xiao, Y.; Zhou, M.; Zeng, M.; Fu, L. Atomic-scale structural modification of 2D materials. *Adv. Sci.* **2019**, 6, 1801501.
20. Hu, W.; Yang, J. Defects in phosphorene. *J. Phys. Chem. C* **2015**, 119, 20474-20480.
21. Pantha, N.; Chauhan, B.; Sharma, P.; Adhikari, N.P. Tuning structural and electronic properties of phosphorene with vacancies. *J. Nepal Phys. Soc.* **2020**, 6, 7-15.
22. Cai, Y.; Chen, S.; Gao, J.; Zhang, G.; Zhang, Y.W. Evolution of intrinsic vacancies and prolonged lifetimes of vacancy clusters in black phosphorene. *Nanoscale* **2019**, 11, 20987-20995.
23. Zhan, F.; Xu, W.; Zou, R.; Yang, J.; Fan, J.; Wu, X.; Wang, R. Interplay of charged states and oxygen dissociation induced by vacancies in phosphorene. *J. Phys. Chem. C* **2019**, 123, 27080-27087.
24. Srivastava, P.; Hembram, K.P.S.S.; Mizuseki, H.; Lee, K.-R.; Han, S.S.; Kim, S. Tuning the electronic and magnetic properties of phosphorene by vacancies and adatoms. *J. Phys. Chem. C* **2015**, 119, 6530-6538.
25. de Sousa, F.E.B.; Araújo, F.R.V.; Farias, G.A.; de Sousa, J.S.; da Costa, D.R. Effects on the electronic properties of multilayer phosphorene due to periodic arrays of vacancies: Band unfolding formalism. *Physica E* **2023**, 152, 115750.
26. Li, J.-x.; Zhang, Q.; Ma, D.-w.; Liu, C.-k.; Li, F. Adsorption properties of CO2, NO2 and SO2 on pristine/defective/non-metallic element doping phosphorene by DFT method. *SSRN Electron. J.* **2024**.
27. Singsen, S.; Watwiangkham, A.; Ngamwongwan, L.; Fongkaew, I.; Jungthawan, S.; Suthirakun, S. Defect Engineering of Green Phosphorene Nanosheets for Detecting Volatile Organic Compounds: A Computational Approach. *ACS Appl. Nano Mater.* **2023**, 6, 1496-1506.

 doi:10.20944/preprints202602.0338.v1

28. Ghadiri, M.; Ghashghaee, M.; Ghambarian, M. Defective phosphorene for highly efficient formaldehyde detection: Periodic density functional calculations. *Phys. Lett. A* **2020**, 384, 126792.
29. Kou, L.; Frauenheim, T.; Chen, C. Phosphorene as a superior gas sensor: Selective adsorption and distinct I-V response. *J. Phys. Chem. Lett.* **2014**, 5, 2675-2681.
30. Donarelli, M.; Ottaviano, L. 2D materials for gas sensing applications: A review on graphene oxide, MoS2, WS2 and phosphorene. *Sensors* **2018**, 18, 3638.
31. Khudair, S.A.M.; Mohaimeed, A.A. Gas Sensor Investigations through Adsorption of Toxic Gas Molecules on Single and Double Vacancy Graphene. *NeuroQuantology* **2020**, 18, 87-95.
32. Qin, Y.; Cao, M.; Lei, M.; Feng, W. First-principles study on the selective gas adsorption of defective SnS. *Vacuum* **2021**, 183, 109792.
33. Corona-García, C.A.; Lucas, H.R.; Ramírez-Pimentel, J.G.; Cruz-Martínez, H.; Cocoletzi, G.H. Adsorption of small pollutant molecules on monolayer aluminum-doped and single-vacancy blue phosphorene. *J. Mol. Model.* **2021**, 27, 141.
34. Soler, J.M.; Artacho, E.; Gale, J.D.; García, A.; Junquera, J.; Ordejón, P.; Sánchez-Portal, D. The SIESTA method for ab initio order-N materials simulation. *J. Phys. Condens. Matter* **2002**, 14, 2745.
35. Zuluaga-Hernandez, E.A.; Flórez, E.; Dorkis, L.; Mora-Ramos, M.E.; Correa, J.D. Small molecule gas adsorption onto blue phosphorene oxide layers. *Appl. Surf. Sci.* **2020**, 530, 147039.
36. Klimeš, J.; Bowler, D.R.; Michaelides, A. Chemical accuracy for the van der Waals density functional. *J. Phys. Condens. Matter* **2009**, 22, 022201.
37. Larsen, A.H.; Mortensen, J.J.; Blomqvist, J.; Castelli, I.E.; Christensen, R.; Dułak, M.; Friis, J.; Groves, M.N.; Hammer, B.; Hargus, C. et al. The atomic simulation environment—a Python library for working with atoms. *J. Phys. Condens. Matter* **2017**, 29, 273002.